Long non-coding RNA metastasis-associated lung adenocarcinoma transcript 1 regulates renal cancer cell migration via cofilin-1

YALI ZHANG[1,2], XINYU GUAN[1,2], HAO WANG[1,2], YONG WANG[3], DAN YUE[4] and RUIBING CHEN[2]

[1]Department of Genetics, School of Basic Medical Sciences, Tianjin Medical University, Tianjin 300070; [2]School of Pharmaceutical Science and Technology, Health Science Platform, Tianjin University, Tianjin 300072; [3]The Second Hospital of Tianjin Medical University, Tianjin Institute of Urology; [4]School of Medical Laboratory, Tianjin Medical University, Tianjin 300070, P.R. China

Received December 3, 2019; Accepted June 23, 2020

DOI: 10.3892/ol.2020.11914

Abstract. Long non-coding RNA (lncRNA) metastasis-associated lung adenocarcinoma transcript 1 (MALAT1) is upregulated in numerous types of cancer, and is implicated in various cellular processes associated with cancer progression. However, the underlying molecular mechanisms by which MALAT1 regulates metastasis remain unclear. The present study investigated the expression of MALAT1 across a range of different cancer types by analyzing RNA sequencing data from The Cancer Genome Atlas database. The results indicate that the expression of MALAT1 is highly tissue-dependent and that MALAT1 is significantly overexpressed in renal clear cell carcinoma (KIRC). The biological role of MALAT1 in regulating KIRC cell migration was further investigated using molecular and cellular assays. The results demonstrate that MALAT1 regulates the expression of cofilin-1 (CFL1), potentially by regulating RNA splicing. MALAT1 knockdown decreased the expression of CFL1 at both the mRNA and protein levels, and affected cytoskeletal rearrangement by regulating the levels of F-actin via CFL1, leading to significantly decreased cellular migration. Clinical analysis confirmed a significant correlation between MALAT1 and CFL1 expression, implicating both genes as biomarkers for poor prognosis in KIRC. The present study demonstrates a novel mechanism by which MALAT1 regulates cell migration, which may be exploited to develop novel therapeutic strategies for managing renal cancer metastasis.

Correspondence to: Professor Ruibing Chen, School of Pharmaceutical Science and Technology, Health Science Platform, Tianjin University, 92 Weijin Road, Nankai, Tianjin 300072, P.R. China
E-mail: rbchen@tju.edu.cn

Abbreviations: RCC, renal cell carcinoma; lncRNA, long non-coding RNA; MALAT1, metastasis-associated lung adenocarcinoma transcript 1; CFL1, cofilin-1; TCGA, The Cancer Genome Atlas; KIRC, renal clear cell carcinoma

Key words: lncRNA, MALAT1, RCC, CFL1, cell migration, cytoskeleton

Introduction

Renal cell carcinoma (RCC) is the seventh most common cancer globally, and alongside an increasing incidence and mortality rate, ~144,000 individuals succumb to the disease each year (1,2). Renal clear cell carcinoma (KIRC) is the most common histological subtype accounting for ~80% of all RCC cases (3), and patients with advanced RCC have a 5-year survival rate of <30% in the United States between 2008 and 2014 (4). Currently, the treatment of RCC remains a major challenge due to the poor response to conventional radiotherapy and chemotherapy (5,6). Therefore, novel therapeutic approaches and diagnostic biomarkers are required to improve the prognosis of patients with RCC.

Long non-coding RNAs (lncRNAs) are a class of mRNA-like transcripts >200 nucleotides in length that lack protein coding capability (7). lncRNAs serve important roles in the regulation of gene expression at multiple levels, including chromatin remodeling, transcriptional regulation, post-transcriptional processing, mRNA translation and protein stability (8). lncRNA dysregulation has been associated with the occurrence and progression of malignant tumors, including lung cancer, cervical cancer and colorectal cancer, by regulating various cellular processes in tumor cells, such as proliferation, migration, differentiation, apoptosis and the cell cycle (9).

Metastasis-associated lung adenocarcinoma transcript 1 (MALAT1), also known as nuclear-enriched abundant transcript 2, was one of the first lncRNA molecules discovered with a designated role in cancer (10,11). The MALAT1 transcript is ~8,000 nucleotides in length and is highly conserved among mammals (12,13). Accumulating evidence has shown that MALAT1 is upregulated in various cancer types, such as lung cancer, esophageal squamous cell carcinoma, gastric cancer, glioma and KIRC, and is reported to promote tumor cell hyperproliferation and metastasis (11,14-17). The nomenclature of MALAT1 is based on its function in regulating lung cancer metastasis; however, the molecular mechanisms underlying the MALAT1-mediated regulation of cell migration are still largely unclear.

A major mechanism by which MALAT1 exerts its biological functions is regulating RNA processing (18). Tripathi *et al* (18) reported that MALAT1 may regulate RNA splicing by interacting with several splicing factors, such as serine/arginine-rich splicing factor 1 and serine/arginine-rich splicing factor 3. A previous study demonstrated that MALAT1 binds multiple subunits of the RNA spliceosome, such as serine/arginine-rich splicing factor 7, ATP-dependent RNA helicase A and splicing factor U2AF2 (19). RNA sequencing conducted by Engreitz *et al* (20) showed that MALAT1 could indirectly interact with a number of pre-mRNAs including pre-cofilin-1 (pre-CFL1) mediated by proteins. CFL1 is an actin binding protein that regulates F-actin severing and depolymerization, a critical step for cytoskeleton dynamics during cellular migration (21,22). A previous study have shown that CFL1 expression is highly associated with cell locomotion and invasion (23). However, to the best of our knowledge, the relationship between MALAT1 and CFL1 has not been investigated, and it is unknown whether CFL1 is an important downstream factor for the regulation of MALAT1-induced cellular migration.

In the present study, we studied the role of MALAT1 in the in the regulation of cell migration in RCC cells and investigated the underlying molecular mechanism.

Materials and methods

Cell culture and transfection. Human renal cancer cell lines ACHN and 786-O were obtained from the American Type Culture Collection. The cells were cultured in Minimum Essential Medium or Dulbecco's modified Eagle's medium (both Corning, Inc.) supplemented with 10% fetal bovine serum (FBS) (Gibco; Thermo Fisher Scientific, Inc.) and 1% penicillin/streptomycin (100 μg/ml) at 37˚C (5% CO_2) in a humidified culture incubator. For small interfering (si)RNA knockdown experiments, MALAT1 siRNA (si-MALAT1-1 and si-MALAT1-2) and scrambled negative control siRNA (Scr) were purchased from Guangzhou RiboBio, Co., Ltd, and the siRNA sequences are displayed in Table SI. Cells cultured in 6-well plates at 40% confluence ($4x10^5$ cells. per plate) were transfected using X-tremeGENE siRNA Transfection Reagent (Roche Diagnostics, Inc.) and were harvested after 48 h of incubation at 37˚C. For rescue experiments, the entire cloned CFL1 sequence (accession number: NM_005507.3) was inserted into the GV358 vector (GeneChem, Inc.). MALAT1 knockdown cells were incubated at 37˚C with 2 μg CFL1 expression plasmid GV358-CFL1 and X-tremeGENE HP DNA Transfection Reagent (Roche Diagnostics, Inc.) and harvested after 36 h.

Reverse transcription-quantitative (RT-q)PCR. Total RNA was isolated from transfected ACHN and 786-O cells using TRIzol® reagent (Invitrogen, Thermo Fisher Scientific, Inc.). For the detection of mRNA, a Fast Quant RT kit (TianGen Biochemical Technology, Co., Ltd.) was used to reverse transcribe 5 μg total RNA into cDNA according to the manufacturer's protocols. The reaction conditions for reverse transcription were: 42˚C for 6 min, 42˚C for 1 h and 95˚C for 10 min. qPCR reactions was performed with the SuperReal SYBR Green PreMix (TianGen Biotech, Co., Ltd.) using a 7500 Fast Real-Time PCR system (Applied Biosystems; Thermo Fisher Scientific, Inc.) and the following reaction conditions: 30 sec at 94˚C, followed by 40 cycles of 5 sec at 94˚C and 1 min at 60˚C. Relative mRNA levels of the target genes were normalized using the reference gene GAPDH and assessed using the $2^{-\Delta\Delta Cq}$ method (24). The primer sequences used for RT-qPCR are displayed in Table SII.

Western blotting. Transiently transfected cells were lysed using 2% sodium dodecyl sulfate (Beijing Solarbio Science and Technology, Co., Ltd.) supplemented with cOmplete™ protease inhibitor cocktail (Roche Diagnostics, Inc.) for 10 min on ice. Total protein was quantified using a BCA quantification kit (Invitrogen; Thermo Fisher Scientific, Inc.). A total of 30 μg protein per lane was loaded onto a 10% gel, resolved using SDS-PAGE and then transferred to activated polyvinylidene difluoride membranes (PVDF) (0.2 μm pore size, EMD Millipore). After blocking with 5% skim milk for 1 h at room temperature (RT), the PVDF membranes were incubated with rabbit anti-human primary antibodies against GAPDH (1:1,000 dilution, cat. no. ab181602, Abcam), β-actin (1:1,000 dilution, cat. no. ab8227, Abcam) or CFL1 (1:1,000 dilution, cat. no. ab42824, Abcam) at 4˚C overnight. After washing with TBST, the blots were incubated with goat anti-rabbit IgG heavy chain (H) + light chain (L) HRP secondary antibody (1:1,000 dilution; cat. no. S0001; Affinity Biosciences) for 1 h at RT. Finally, the blots were developed using enhanced chemiluminescence luminol reagents (Pierce; Thermo Fisher Scientific, Inc.) and the protein bands were analyzed using ImageJ software version 1.8.0 (National Institutes of Health).

Clinical specimens. To investigate the expression of MALAT1 and CFL1 using RT-qPCR in human RCC tissues, 20 malignant renal cancer tissue specimens were collected from 15 male and 5 female patients (median age, 65 years; age range, 45-75 years). The tissues were surgically removed at the Second Hospital of Tianjin Medical University with written consent from the patients, and with approval from the Tianjin Medical University Second Hospital Medical Ethics Committee (Tianjin, China). All patients received radical nephrectomy with no preoperative or postoperative adjuvant therapy. No additional inclusion or exclusion criteria were used. All specimens were evaluated by two experienced pathologists independently to ensure that they were correctly identified as KIRC. Diagnostic criteria for KIRC include grossly circumscribed mass, sheets and nests of cells surrounded by extensive capillary network, predominantly composed of clear cells, nuclei ranging from round and regular at low grade to pleomorphic at high grade, dysplasia of adjacent non-carcinomatous tubules in some cases, and multiple and/or familial clear cell carcinomas may be seen in von Hippel Lindau syndrome (25). The collected tumor tissues were frozen in liquid nitrogen immediately and stored at -80˚C. Clinicopathological information of the patients is presented in Table SIII.

Confocal imaging. Renal cancer cells were plated at $3x10^4$ per well into 12-well plates containing sterile glass coverslips. After incubation for 24 h at 37˚C, the cells were fixed with 4% paraformaldehyde at RT for 10 min and permeabilized with 0.2% Triton X-100 (Beijing Solarbio Science and Technology,

Co., Ltd.) for 10 min. After being washed three times with phosphate buffered saline (PBS), the cells were blocked with 3% bovine serum albumin (Beijing Solarbio Science and Technology, Co., Ltd.) for 1 h at RT. Next, the cells were incubated with rhodamine conjugated phalloidin (Invitrogen; Thermo Fisher Scientific, Inc.) for 30 min at RT. After being washed three times with PBS, cell nuclei were stained with 4',6-diamidino-2-phenylindole for 10 min at RT. The stained cells were visualized using confocal laser scanning microscopy at x400 magnification (Olympus Corporation).

Actin polymerization assay. Renal cancer cells were seeded at $3x10^5$ cells per well in 6-well plates. After incubation for 24 h at 37˚C, the cells were fixed with 4% paraformaldehyde at RT for 10 min, permeabilized with 0.1% Triton X-100 for 20 min at RT, and then washed three times with F-actin buffer (10 mM HEPES, 20 mM KH_2PO_4, 5 mM EGTA and 2 mM $MgCl_2$). Next, the cells were incubated with rhodamine conjugated phalloidin (dilution, 1:40; cat. no. R415; Thermo Fisher Scientific, Inc.) at RT for 60 min. Phalloidin was extracted using 100% methanol, and the fluorescence intensity was quantified using a microplate reader (BioTek Instruments, Inc.).

Wound healing assay. Following 48 h transfection, ACHN and 786-O cells were cultured in 6-well plates until confluent. The cells were scratched in the middle of the plate using a 10 μl sterile pipette tip and washed three times with PBS to remove detached cells and debris. The cells were cultured in medium containing 1% FBS for an additional 24 h. Images were captured at 0 and 24 h, and the migration distance was measured at 200x magnification using a light microscope (Olympus Corporation).

Invasion assay. An invasion assay was performed using 24-well Transwell chambers (Corning, Inc.) containing polycarbonate membranes (pore size, 8 μm) precoated with Matrigel at 37˚C for 30 min (BD Biosciences). After starvation overnight, $1x10^5$ transfected cells in 200 μl serum-free medium were loaded into the upper chambers, and 600 μl medium containing 10% FBS was added to the lower chambers as a chemoattractant. After incubation for 24 h at 37˚C, non-invasive cells on the upper membrane surface were removed with wet cotton swabs, and the cells that had invaded to the lower membrane surface were fixed with 4% paraformaldehyde at RT (Beijing Solarbio Science and Technology, Co., Ltd.) and stained with 0.01% crystal violet solution (Sigma-Aldrich; Merck KGaA) at RT for 10 min. The migratory cells were counted manually in six randomly selected regions at 200x magnification using a light microscope (Olympus Corporation).

Bioinformatics analysis. Gene expression and clinical data were obtained from The Cancer Genome Atlas (TCGA) database (https://www.cancer.gov/tcga) via the TCGAbioLinks version 2.12.2 (26) Bioconductor R package in R (27) by RStudio (version 3.6.0) (28). The following tumor types were selected: Bladder urothelial carcinoma (BLCA), breast invasive carcinoma (BRCA), colon adenocarcinoma (COAD), esophageal carcinoma, glioblastoma multiforme, head and neck squamous cell carcinoma (HNSC), KIRC, renal papillary cell carcinoma (KIRP), liver hepatocellular carcinoma (LIHC), lung adenocarcinoma, lung squamous cell carcinoma (LUSC), pancreatic adenocarcinoma, pheochromocytoma and paraganglioma, prostate adenocarcinoma (PRAD), rectum adenocarcinoma (READ), sarcoma, skin cutaneous melanoma, stomach adenocarcinoma (STAD), thyroid carcinoma, thymoma (THYM) and uterine corpus endometrial carcinoma. The raw read counts per gene of the gene expression data were normalized to Transcripts Per Million (29). Differential expression analyses of MALAT1 and CFL1 between tumor and normal samples were conducted using the ggplot2 version 3.2.0 (http://ggplot2.tidyverse.org) package integrated with ggpubr version 0.2.1 (https://rpkgs.datanovia.com/ggpubr/) package in R. Gene Ontology (GO) and Kyoto Encyclopedia of Genes and Genomes (KEGG) pathway enrichment analysis were conducted by clusterProfiler R/bioconductor package (v3.12.0) (30) in R.

Statistical analysis. Prism version 7.0 (GraphPad Software, Inc.) was used to plot mean and standard deviation data. Statistical analysis was performed by two-tailed unpaired Student's t-test between two groups or one-way analysis of variance followed by Tukey's post hoc test between multiple groups. Wilcoxon rank-sum test was used for statistical analysis of TCGA data, when patients were stratified into high expression group and low expression group, based on the 33 and 66 percentiles of the two RNAs (low, 1-33 percentile; high, 66-100 percentile). Overall survival (OS) analysis was performed using the survival R package version 2.43.3 (https://github.com/therneau/survival). Survival analysis was performed using the Kaplan-Meier method and compared using the log-rank test. The correlation between *MALAT1* and *CFL1* mRNA expression was evaluated using Pearson's coefficient. $P<0.05$ was considered to indicate a statistically significant difference.

Results

Pan-cancer analysis of MALAT1 expression. To acquire the expression pattern of MALAT1 across different cancer types, RNA sequencing datasets from 21 of the most common types of cancer were obtained from TCGA database. The results indicated that MALAT1 is significantly upregulated in eight different types of cancer compared with normal tissues, including COAD (3-fold change, $P<0.001$), HNSC (1.6-fold change, $P<0.001$), KIRC (2.1-fold change, $P<0.001$), KIRP (1.2-fold change, $P=0.041$); LIHC (2.9-fold change, $P<0.001$), PRAD (1.5-fold change, $P<0.001$), READ (2.4-fold change, $P=0.01$) and STAD (fold-change: 1.7; $P=0.003$). KIRC was one of the cancer types with the most significant upregulation of MALAT1. Surprisingly, MALAT1 was also decreased in three types of cancer: BLCA (0.7-fold change, $P=0.032$), BRCA (0.9-fold change; $P=0.004$) and LUSC (0.8-fold change, $P=0.036$) (all Fig. 1). The expression of MALAT1 was not significantly changed in the other ten types of cancer. These results suggest that the expression of MALAT1 is cancer type-dependent and may play distinct biological roles in different types of cancer.

Functional analysis of MALAT1 binding pre-mRNAs. MALAT1 is a major component of nucleus speckles (18)

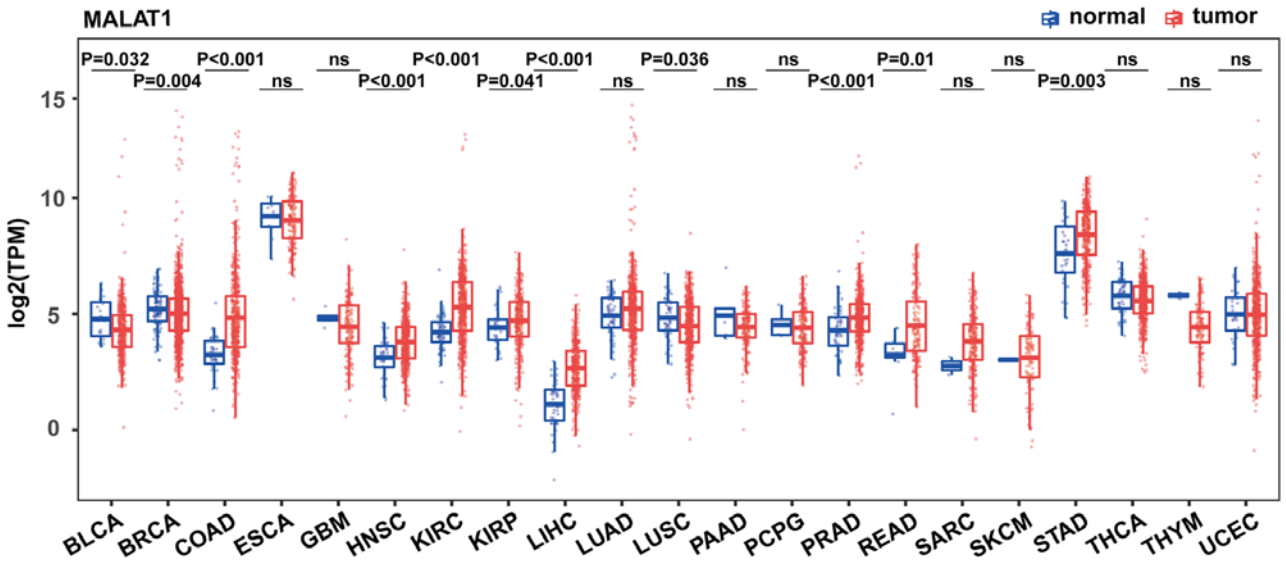

Figure 1. Comparison of MALAT1 expression in tumors and corresponding normal tissues from TCGA. Expression of MALAT1 was measured using $\log_2$(TPM). Wilcoxon rank-sum test was used for statistical analysis and the data were not paired. MALAT1, metastasis-associated lung adenocarcinoma transcript 1; TPM, Transcripts Per Million; TCGA, The Cancer Genome Atlas; BLCA, bladder urothelial carcinoma; BRCA, breast invasive carcinoma; COAD, colon adenocarcinoma; ESCA, esophageal carcinoma; GBM, glioblastoma multiforme; HNSC, head and neck squamous cell carcinoma; KIRC, clear cell kidney carcinoma; KIRP, kidney renal papillary cell carcinoma; LIHC, liver hepatocellular carcinoma; LUAD, lung adenocarcinoma; LUSC, lung squamous cell carcinoma; PAAD, pancreatic adenocarcinoma; PCPG, pheochromocytoma and paraganglioma; PRAD, prostate adenocarcinoma; READ, rectum adenocarcinoma; SARC, sarcoma; SKCM, skin cutaneous melanoma; STAD, stomach adenocarcinoma; THCA, thyroid carcinoma; THYM, thymoma; UCEC, uterine corpus endometrial carcinoma; ns, not significant.

and indirectly binds with a number of pre-mRNAs through protein intermediates, thereby regulating pre-mRNA expression through RNA splicing (20). To better understand the biological function of MALAT1, GO and KEGG pathway enrichment analysis was performed on the pre-mRNAs that were identified to bind with MALAT1. Functional enrichment analysis revealed that the top-ranked biological processes included 'mRNA processing' and 'RNA splicing' (Fig. S1A). KEGG pathway enrichment analysis showed that pre-mRNAs that bound to MALAT1 were significantly enriched in 'spliceosome' pathways with the highest protein count as 20 (Fig. S1B). This result further supports the role of MALAT1 in RNA splicing. Pre-*CFL1* mRNA also had a marked enrichment among the 488 observed pre-mRNAs (fold-19.79 enrichment) (20). CFL1 is a critical modulator of cytoskeleton rearrangement during cell migration (21,22), and the present findings suggest that MALAT1 may be directly involved in cell migration by regulating pre-*CFL1* splicing.

MALAT1 regulates the expression of CFL1. Next, the association between MALAT1 and CFL1 was examined. MALAT1 siRNA knockdown was investigated in ACHN and 786-O cells, and MALAT1 downregulation of was subsequently confirmed using RT-qPCR (Fig. 2A and B). MALAT1 knockdown inhibited CFL1 expression at both the mRNA and protein levels compared with respective control cells in both ACHN (Fig. 2A) and 786-O cells. (Fig. 2B). si-MALAT1-2 had a higher knockdown efficiency compared with si-MALAT1-1 and was used for the following experiments. In addition, levels of pre-*CFL1* mRNA were examined using primers that targeted the junction of the first exon and intron (Fig. 2C). Knockdown of MALAT1 decreased the levels of *CFL1* mRNA in both ACHN (P<0.001, Fig. 2D) and 786-O cells (P=0.008; Fig. 2E) but not pre-*CFL1*. Taken together, these results suggest that MALAT-knockdown inhibits CFL1 expression at both the RNA and protein level by post-transcriptional regulation.

MALAT1-knockdown elevates F-actin accumulation. To establish how MALAT1 modulates the cytoskeleton through CFL1, the overexpression efficiency of *CFL1* plasmid in ACHN was first evaluated (at mRNA level, P<0.001; at protein level, P=0.003; Fig. S2A) and 786-O cells (at mRNA level, P=0.004; at protein level, P<0.001; Fig. S2B). Then, rescue experiments were performed by first knocking down MALAT1 with siRNA and then overexpressing CFL1. The efficiency of transfection was evaluated using RT-qPCR and western blotting in both ACHN (Fig. 3A) and 786-O cells (Fig. 3B). Western blotting showed that MALAT1 knockdown did not affect the total amount of β-actin (Fig. 3C). A fluorescence staining assay was performed to measure the levels of F-actin in the cells and observed marked accumulation of F-actin near the cell membrane in MALAT1 knockdown cells as compared with the corresponding control cells (Fig. 3D). To verify that the accumulation of F-actin was mediated by CFL1, a rescue experiment was performed in MALAT1-knockdown cells with the CFL1 vector. Restoring the expression of CFL1 in MALAT1-knockdown cells decreased F-actin accumulation to a similar level as the control cells. In addition, the levels of F-actin in the cells were quantified and showed a consistent result with the fluorescence staining assay (Fig. 3A-D). Knockdown of MALAT1 significantly increased the level of F-actin, which was reduced to control levels in rescued cells (Fig. 3E). Taken together, these results demonstrate that MALAT1-knockdown inhibited F-actin depolymerization and induced F-actin accumulation near the cell membrane thorough suppressing CFL1 expression.

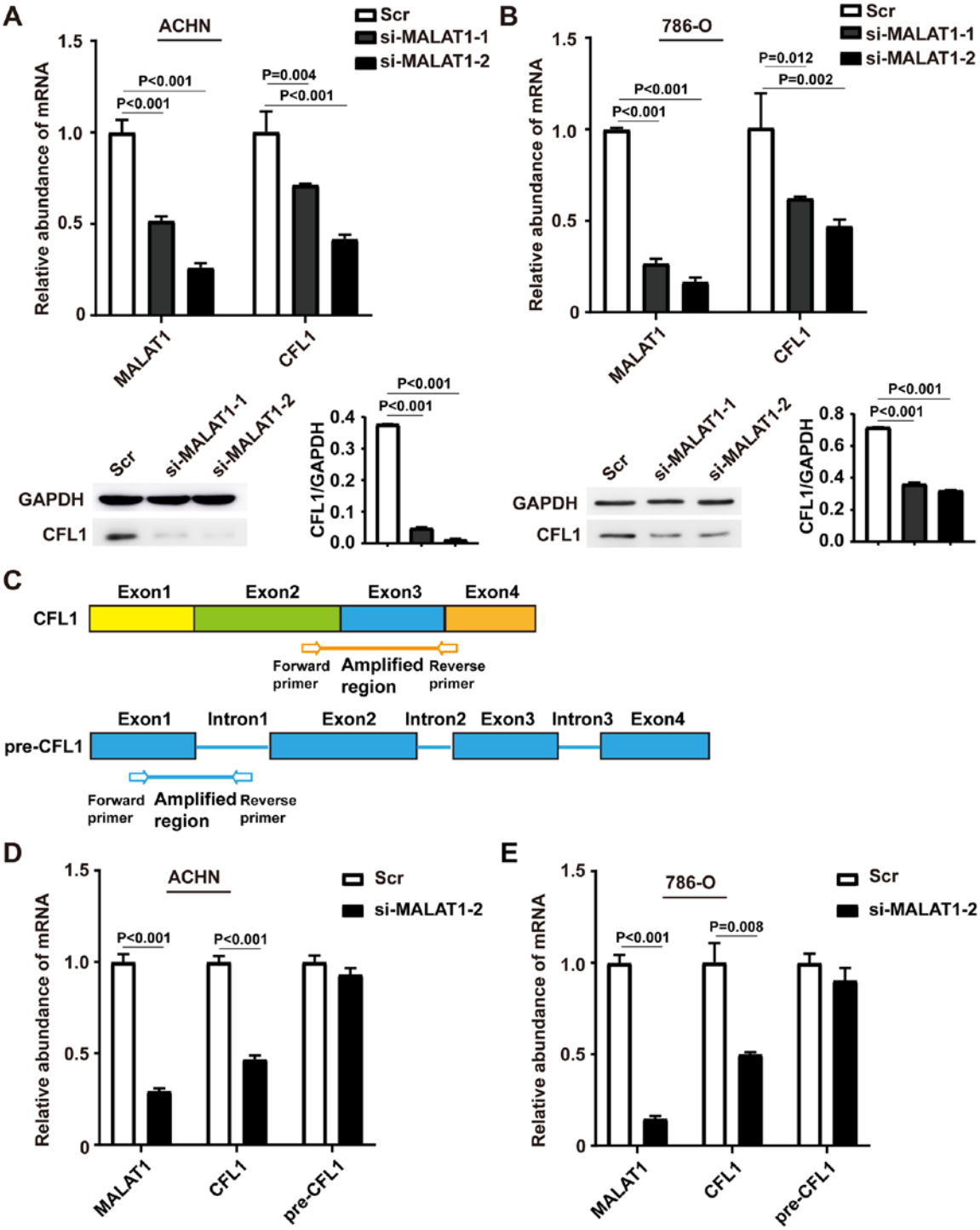

Figure 2. MALAT1-knockdown inhibits CFL1 expression in KIRC cells. RT-qPCR and western blotting analyses of CFL1 expression in MALAT1-downregulated (A) ACHN and (B) 786-O cells and their corresponding control cells. The data are expressed as mean ± SD (n=3) and one-way analysis of variance followed by Tukey's post hoc test was used for statistical analysis. (C) Amplified regions of *CFL1* and pre-*CFL1* mRNAs. RT-qPCR analysis of *CFL1* and pre-*CFL1* mRNA expression levels in MALAT1 downregulated (D) ACHN and (E) 786-O cells and their corresponding control cells. The data were expressed as mean ± SD (n=3) and unpaired Student's t-test was used for statistical analysis. MALAT1, metastasis-associated lung adenocarcinoma transcript 1; CFL1, cofilin-1; KIRC, kidney renal clear cell carcinoma; SD, standard deviation; Scr, scramble; si, small interfering; RT-qPCR, reverse transcription-quantitative PCR.

MALAT1 regulates the migration and invasiveness of RCC cells through CFL1. To determine whether MALAT1 is required for the migration and invasion of RCC cells, the effect of MALAT1-knockdown was examined in ACHN and 786-O cells using cellular migration assays. In the wound assay, 1% FBS was used to sustain cell vitality. MALAT1 siRNA knockdown inhibited the migration and invasiveness of RCC cells compared with their corresponding control cells. To confirm the role of CFL1 in MALAT1-mediated cell mobility, the expression of CFL1 in MALAT-knockdown cells was restored, and showed that the migration and invasion capacities of these cells were elevated to similar levels as in the corresponding control cells (Fig. 4). Taken together, these results suggest that MALAT1 downregulation inhibits RCC cell migration and invasiveness through CFL1.

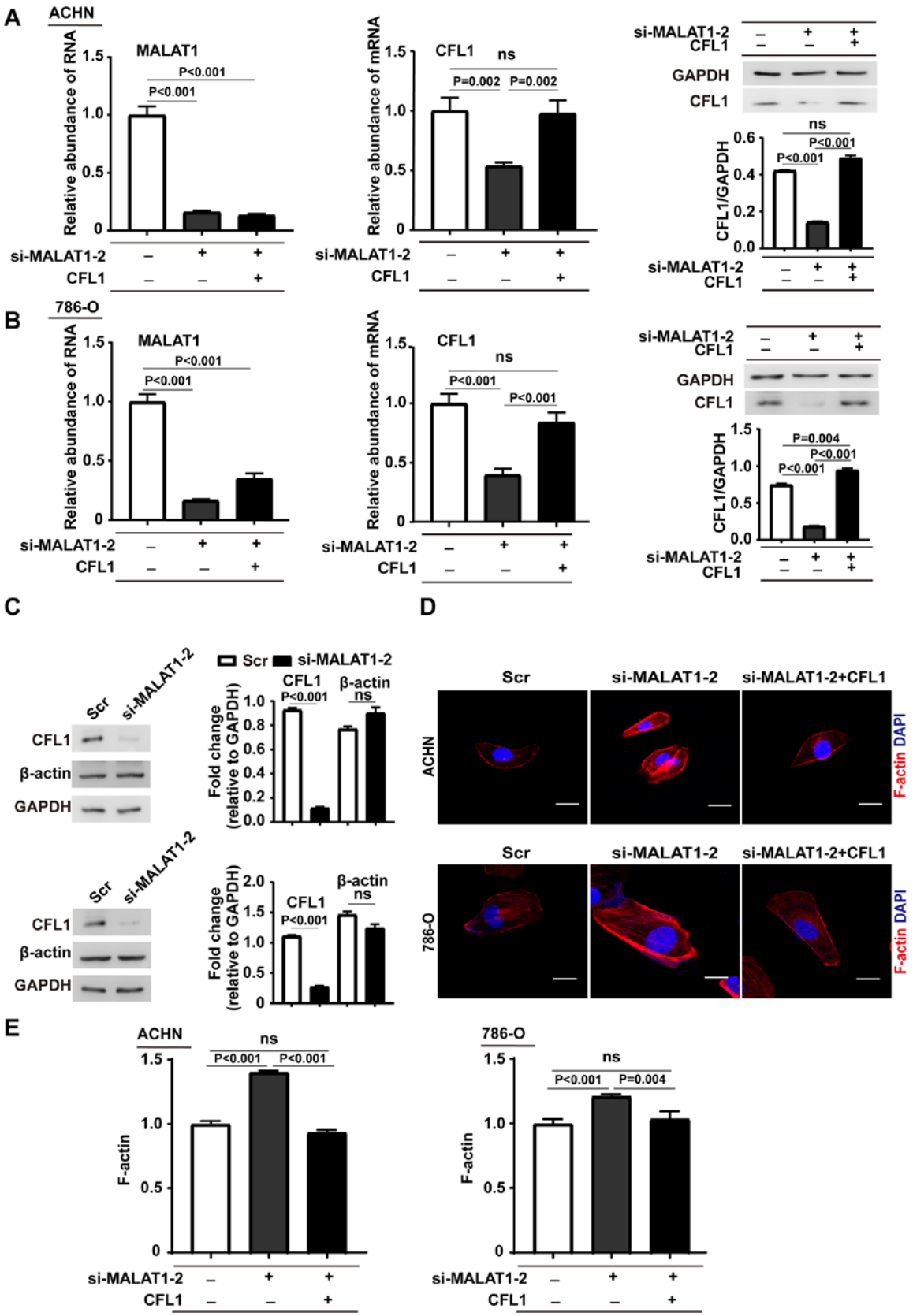

Figure 3. Reverse transcription-quantitative PCR and western blotting analyses of CFL1 in MALAT1-downregulated (A) ACHN and (B) 786-O cells transfected with CFL1 plasmids and the corresponding control cells. The data are presented as the mean ± SD (n=3) and one-way ANOVA followed by Tukey's post hoc test was used for statistical analysis. (C) Western blots of CFL1 and β-actin in MALAT1-downregulated ACHN (upper panel) and 786-O (lower panel) cells and their corresponding control cells. Data are shown as mean ± SD (n=3) and unpaired Student's t-test was used for statistical analysis. (D) Confocal imaging of cellular F-actin in cells transfected with MALAT1 siRNA or MALAT1 siRNA and CFL1 vector. F-actin was stained with rhodamine conjugated phalloidin. Upper panel, ACHN; lower panel, 786-O. Scale bar, 20 μm. (E) Quantification of F-actin levels using an actin polymerization assay in cells transfected with MALAT1 siRNA or MALAT1 siRNA and CFL1 vector. F-actin was stained with rhodamine conjugated phalloidin. Data are expressed as mean ± SD (n=3) and one-way ANOVA followed by Tukey's post hoc test was used for statistical analysis. MALAT1, metastasis-associated lung adenocarcinoma transcript 1; ns, not significant; CFL1, cofilin-1; SD, standard deviation; Scr, scramble; si, small interfering; ANOVA, analysis of variance.

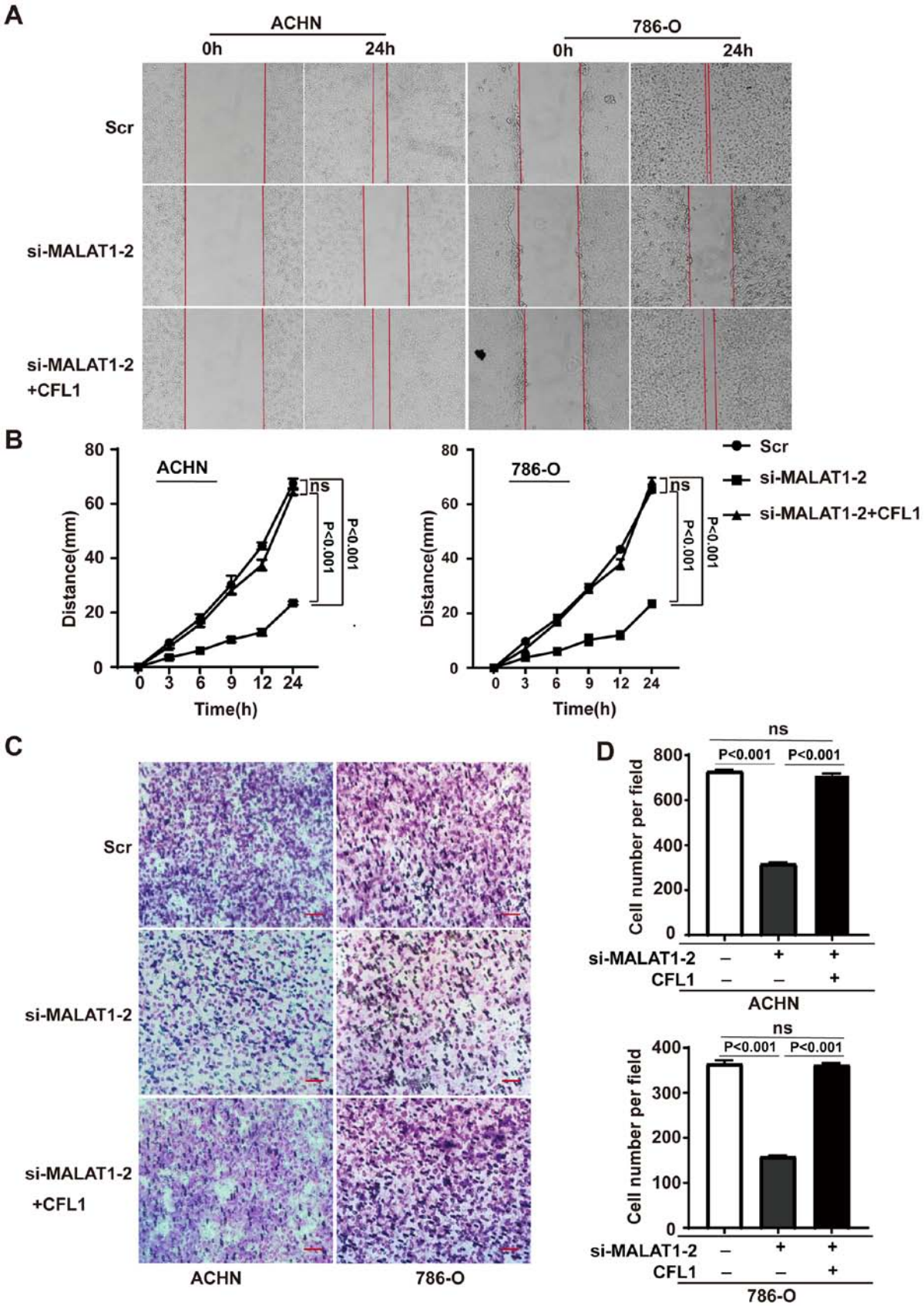

Figure 4. MALAT1 regulates the migration and invasion of renal cell carcinoma cells through CFL1. (A) Cell migration assay of siMALAT1 cells and cells transfected with both siMALAT1 and CFL1 vector. Left panel, ACHN; right panel, 786-O. Representative images of the cells at 0 and 24 h are shown. Magnification, x100. (B) Quantification of cell migration assay. Migration distances are shown as the mean ± SD of three independent analyses, and one-way ANOVA followed by Tukey's post hoc test was used for statistical analysis. Left panel, ACHN; right panel, 786-O. (C) Invasion assay of the kidney renal clear cell carcinoma cells with indicated treatments. Left panel, ACHN; right panel, 786-O. Representative images are shown. Magnification, x200. Scale bar, 100 μm. (D) Quantification of the invasion assay. Results are shown as the mean ± SD of three independent analyses and one-way ANOVA followed by Tukey's post hoc test was used for statistical analysis Upper panel, ACHN; lower panel, 786-O. ns, not significant; MALAT1, metastasis-associated lung adenocarcinoma transcript 1; si, small interfering; CFL1, cofilin-1; SD, standard deviation; ANOVA, analysis of variance.

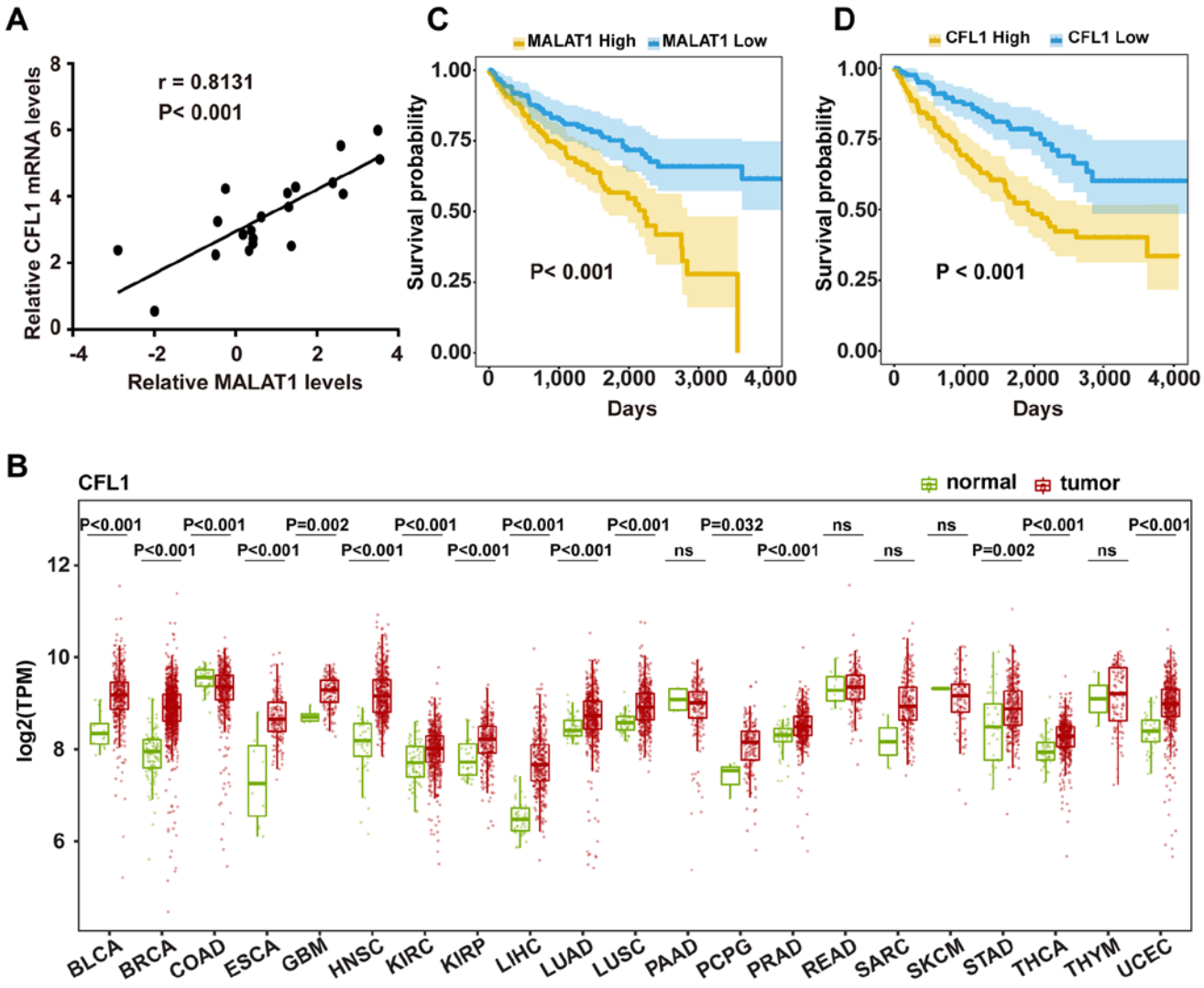

Figure 5. Correlation and survival analyses of MALAT1 and CFL1 expression. (A) Correlation between *MALAT1* and *CFL1* mRNA expression in RCC tissues. The data were expressed as mean ± SD (n=20). (B) Comparison of CFL1 expression in tumors and corresponding normal tissues. Expression of CFL1 was measured using log2(TPM). Data were obtained from TCGA database, and the data were not paired. Wilcoxon rank-sum test was used for statistical analysis. Kaplan-Meier survival analysis of (C) *MALAT1* and (D) *CFL1* mRNA in patients with KIRC from TCGA database using log-rank test. Patients were stratified into high expression group and low expression group based on the 33 and 66 percentiles of the two RNAs (low, 1-33 percentile; high, 66-100 percentile). ns, not significant; MALAT1, metastasis-associated lung adenocarcinoma transcript 1; CFL1, cofilin-1; SD, standard deviation; TPM, Transcripts Per Million; TCGA, The Cancer Genome Atlas; BCLA, bladder urothelial carcinoma; BRCA, breast invasive carcinoma; COAD, colon adenocarcinoma, HNSC, esophageal carcinoma, glioblastoma multiforme, head and neck squamous cell carcinoma; KIRC, clear cell kidney carcinoma; KIRP, renal papillary cell carcinoma; LIHC, liver hepatocellular carcinoma; LUAD, lung adenocarcinoma; LUSC, lung squamous cell carcinoma; PAAD, pancreatic adenocarcinoma; PCPG, pheochromocytoma and paraganglioma; PRAD, prostate adenocarcinoma; READ rectum adenocarcinoma; SARC, sarcoma; STAD, skin cutaneous melanoma, stomach adenocarcinoma; THCA, thyroid carcinoma; THYM, thymoma; UCEC, uterine corpus endometrial carcinoma.

Clinical analyses of MALAT1 and CFL1. Finally, the clinical implications of MALAT1 and CFL1 were investigated. Levels of *MALAT1* and *CFL1* mRNA were analyzed using RT-qPCR in 20 KIRC tumor tissues. The results showed a positive correlation (r=0.8131, P<0.001) between *MALAT1* and *CFL1* (Fig. 5A), which further confirmed the present hypothesis. By analyzing the mRNA sequencing data from TCGA database, it was found that the levels of *CFL1* mRNA were significantly increased in 15 common types of cancer, including KIRC (1.2-fold change; P<0.001) and significantly decreased only in COAD (P<0.001) as compared with the normal tissues (Fig. 5B). In addition, Kaplan-Meier survival analyses revealed that both MALAT1 (P<0.001) and CFL1 (P<0.001) were associated with poor overall survival time in patients with KIRC (Fig. 5C and D). Taken together, these data suggest that *MALAT1* and *CFL1* expression are positively correlated in KIRC tumor tissues, and that both *MALAT1* and *CFL1* were upregulated and associated with poor prognosis.

Discussion

In the past decade, lncRNA MALAT1 has been implicated in the progression of several cancer types, including lung cancer, bladder cancer, hepatocellular carcinoma and cervical cancer (11,12,31-35). Most studies have highlighted the pro-oncogenic role of MALAT1; however, it is shown to suppress tumor progression in some cancer types. The pan-cancer analysis performed in the present study

showed that the expression levels of MALAT1 increase in the majority of cancer types, but is downregulated in several types, such as BRCA and LUSC. A recent study showed that MALAT1 inhibits breast cancer metastasis by binding and inactivating the pro-metastatic transcription factor TEAD (36). Additionally, an earlier study revealed that MALAT1 expression in metastatic adenocarcinoma is several folds higher compared with that in non-metastatic adenocarcinoma, but that the relative expression is decreased in squamous cell carcinomas (12). These studies indicate that the roles of MALAT1 may be cancer type- and histological subtype-dependent.

A number of studies have demonstrated that MALAT1 functions in the regulation of different hallmarks of cancer, especially cell proliferation and apoptosis. For example, MALAT1 promoted cell proliferation and inhibited apoptosis by suppressing tumor necrosis factor receptor-associated factor 6 expression via sponging microRNA (miR)-146b-5p in hepatocellular carcinoma (37). It was also reported that MALAT1 regulated cellular proliferation and apoptosis by binding to unmethylated polycomb 2 protein and promoting E2F1 SUMOylation (38). A previous study also demonstrated that MALAT1 promotes cell proliferation and inhibits apoptosis by suppressing p53 activation (19). Overall, these studies suggest that MALAT1 may be involved in various tumor-associated cellular processes via distinct mechanisms.

The underlying mechanism by which MALAT1 regulates the metastatic phenotype of different types of cancer is still largely unclear (11,14-17). Several studies have demonstrated the role of MALAT1 in epithelial-mesenchymal transition (EMT). For example, MALAT1 is reported to promote EMT by sponging miR-126-5p and thereby increasing the expression of metastasis-associated molecules, such as vascular endothelial growth factor A, snail family transcriptional repressor 2 and twist family bHLH transcription factor 1 in colorectal cancer (39). Hirata *et al* (32) also reported that MALAT1 promoted cell invasion through interacting with enhancer of zeste 2 polycomb repressive complex 2 subunit and inhibited E-cadherin expression (32). In our previous study, MALAT1 mediated tumor growth by regulating the activity of p53 (19). However, it is unknown whether MALAT1 can directly act on the cytoskeleton. In the present study, MALAT1 knockdown decreased CFL1 expression at both the mRNA and protein level without affecting the abundance of its pre-mRNA. A possible explanation for this is that MALAT1 regulates the alternative splicing of pre-*CFL1*, resulting in higher levels of unstable CFL1 transcripts that are immediately degraded. In an ongoing project in the School of Basic Medical Sciences at Tianjin Medical University, it was observed that MALAT knockdown markedly affected the landscape of alternative splicing (data not shown). However, the pool of pre-mRNA is affected by three factors; transcription, degradation and splicing (40). Further evidence is required to determine the contribution of each of these factors in the results of the present study, by experiments such as RNA sequencing.

CFL1 is a critical molecule that regulates cytoskeletal dynamics by depolymerizing actin filaments, and is required for cytokinesis and cell movement (21,23,41), while the loss of CFL1 increases F-actin accumulation (42). Although a previous study implicated CFL1 in cell proliferation (43),

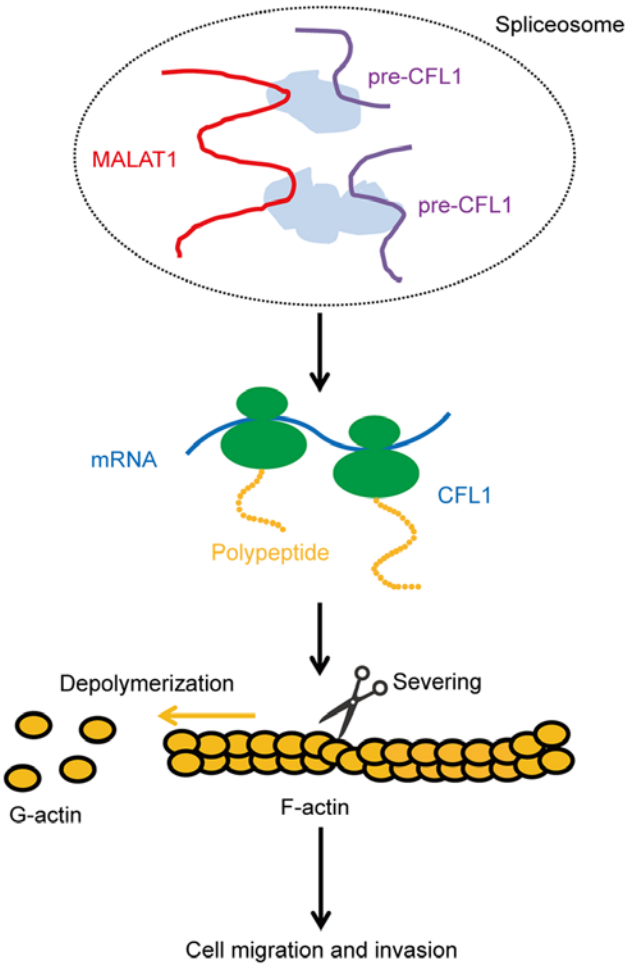

Figure 6. Proposed molecular mechanism by which MALAT1 regulates cell migration and invasion via CFL1. MALAT1, metastasis-associated lung adenocarcinoma transcript 1; CFL1, cofilin-1.

substantial research has showed that CFL1 is more directly associated with the cytoskeleton and cell migration (21,23,41). Therefore, the role of CFL1 in cell migration was the focus of the present study. Furthermore, Wang *et al* (22) demonstrated that CFL1 was associated with cell invasion and cancer metastasis. The present data demonstrated that MALAT1 promotes cell migration and invasion by modulating the level of F-actin through regulation of the expression of CFL1 in RCC cells (Fig. 6).

In conclusion. the present study identified a novel mechanism by which MALAT1 regulates RCC cell migration and invasion. TCGA database and RT-qPCR analyses further demonstrated a positive correlation between MALAT1 and CFL1. Moreover, increased expression of these two molecules in RCC tumor tissues were associated with poorer overall patient survival. Functional and mechanistic analyses suggested that MALAT1 knockdown inhibited renal cancer cell migration by inhibiting CFL1 expression. These findings may provide a potentially novel therapeutic target for RCC treatment.

Acknowledgements

Not applicable.

Funding

The present study was supported by grants from The National Natural Science Foundation of China (grant nos. 21974094, 21575103, 81872078 and 81772945); The Natural Science Foundation of Tianjin (grant nos. 18JCYBJC25200 and 18JC YBJC26700), the Young Elite Scientists Sponsorship Program (grant no. TJSQNTJ-2017-10) and the Scientific Research Foundation for the Returned Overseas Chinese Scholars (grant no. 2016015).

Availability of data and materials

The datasets used and/or analyzed during the present study are available from the corresponding author on reasonable request or available in The Cancer Genome Atlas repository, https://www.cancer.gov/tcga.

Authors' contributions

YLZ wrote the manuscript and conducted experiments; XG assisted in performing the experiments. RBC designed the study and revised the manuscript. HW and XG analyzed and interpreted the data. YW and DY collected the tumor tissues and processed the samples for RT-qPCR analysis, and also assisted in writing and revising the manuscript. All authors read and approved the final manuscript.

Ethics approval and consent to participate

Tianjin Medical University Second Hospital Medical Ethics Committee (Tianjin, China) approved the present study (approval no. KY2020K019) and all participants provided written informed consent for opt-in.

Patient consent for publication

Not applicable.

Competing interests

The authors declare that they have no competing interests.

References

1. Ferlay J, Soerjomataram I, Dikshit R, Eser S, Mathers C, Rebelo M, Parkin DM, Forman D and Bray F: Cancer incidence and mortality worldwide: Source, methods and major patterns in GLOBOCAN 2012. Int J Cancer 136: E359-E386, 2015.
2. Siegel RL, Miller KD and Jemal A: Cancer statistics 2017. CA Cancer J Clin 67: 7-30, 2017.
3. Lopez-Beltran A, Carrasco JC, Cheng L, Scarpelli M, Kirkali Z and Montironi R: 2009 update on the classification of renal epithelial tumours in adults. Int J Urol 16: 432-443, 2009.
4. Siegel RL, Miller KD and Jemal A: Cancer statistics, 2019. CA Cancer J Clin 69: 7-34, 2019.
5. Bedke J, Gauler T, Grünwald V, Hegele A, Herrmann E, Hinz S, Janssen J, Schmitz S, Schostak M, Tesch H, *et al*: Systemic therapy in metastatic renal cell carcinoma. World J Urol 35: 179-188, 2017.
6. Brown C: Targeted therapy: An elusive cancer target. Nature 537: S106-S108, 2016.
7. Ulitsky I and Bartel DP: LincRNAs: Genomics, evolution, and mechanisms. Cell 154: 26-46, 2013.
8. Yang L, Lin C, Jin C, Yang JC, Tanasa B, Li W, Merkurjev D, Ohgi KA, Meng D, Zhang J, *et al*: LncRNA-dependent mechanisms of androgen receptor-regulated gene activation programs. Nature 500: 598-602, 2013.
9. Wilusz JE: Long noncoding RNAs: Re-writing dogmas of RNA processing and stability. Biochim Biophys Acta 1859: 128-138, 2016.
10. Gutschner T, Hämmerle M and Diederichs S: MALAT1-a paradigm for long noncoding RNA function in cancer. J Mol Med (Berl) 91: 791-801, 2013.
11. Gutschner T, Hämmerle M, Eissmann M, Hsu J, Kim Y, Hung G, Revenko A, Arun G, Stentrup M, Gross M, *et al*: The noncoding RNA MALAT1 is a critical regulator of the metastasis phenotype of lung cancer cells. Cancer Res 73: 1180-1189, 2013.
12. Ji P, Diederichs S, Wang W, Böing S, Metzger R, Schneider PM, Tidow N, Brandt B, Buerger H, Bulk E, *et al*: MALAT-1, a novel noncoding RNA, and thymosin beta4 predict metastasis and survival in early-stage non-small cell lung cancer. Oncogene 22: 8031-8041, 2003.
13. Guttman M, Amit I, Garber M, French C, Lin MF, Feldser D, Huarte M, Zuk O, Carey BW, Cassady JP, *et al*: Chromatin signature reveals over a thousand highly conserved large non-coding RNAs in mammals. Nature 458: 223-227, 2009.
14. Hu L, Wu Y, Tan D, Meng H, Wang K, Bai Y and Yang K: Up-regulation of long noncoding RNA MALAT1 contributes to proliferation and metastasis in esophageal squamous cell carcinoma. J Exp Clin Cancer Res 34: 7, 2015.
15. Okugawa Y, Toiyama Y, Hur K, Toden S, Saigusa S, Tanaka K, Inoue Y, Mohri Y, Kusunoki M, Boland CR and Goel A: Metastasis-associated long non-coding RNA drives gastric cancer development and promotes peritoneal metastasis. Carcinogenesis 35: 2731-2739, 2014.
16. Park JY, Lee JE, Park JB, Yoo H, Lee SH and Kim JH: Roles of long non-coding RNAs on tumourigenesis and glioma development. Brain Tumour Res Treat 2: 1-6, 2014.
17. Xiao H, Tang K, Liu P, Chen K, Hu J, Zeng J, Xiao W, Yu G, Yao W, Zhou H, *et al*: LncRNA MALAT1 functions as a competing endogenous RNA to regulate ZEB2 expression by sponging miR-200s in clear cell kidney carcinoma. Oncotarget 6: 38005-38015, 2015.
18. Tripathi V, Ellis JD, Shen Z, Song DY, Pan Q, Watt AT, Freier SM, Bennett CF, Sharma A, Bubulya PA, *et al*: The nuclear-retained noncoding RNA MALAT1 regulates alternative splicing by modulating SR splicing factor phosphorylation. Mol Cell 39: 925-938, 2010.
19. Chen R, Liu Y, Zhuang H, Yang B, Hei K, Xiao M, Hou C, Gao H, Zhang X, Jia C, *et al*: Quantitative proteomics reveals that long non-coding RNA MALAT1 interacts with DBC1 to regulate p53 acetylation. Nucleic Acids Res 45: 9947-9959, 2017.
20. Engreitz JM, Sirokman K, McDonel P, Shishkin AA, Surka C, Russell P, Grossman SR, Chow AY, Guttman M and Lander ES: RNA-RNA interactions enable specific targeting of noncoding RNAs to nascent pre-mRNAs and chromatin sites. Cell 159: 188-199, 2014.
21. Dawe HR, Minamide LS, Bamburg JR and Cramer LP: ADF/cofilin controls cell polarity during fibroblast migration. Curr Biol 13: 252-257, 2003.
22. Wang W, Eddy R and Condeelis J: The cofilin pathway in breast cancer invasion and metastasis. Nat Rev Cancer 7: 429-440, 2007.
23. Bravo-Cordero JJ, Magalhaes MA, Eddy RJ, Hodgson L and Condeelis J: Functions of cofilin in cell locomotion and invasion. Nat Rev Mol Cell Biol 14: 405-415, 2013.
24. Livak KJ and Schmittgen TD: Analysis of relative gene expression data using real-time quantitative PCR and the 2(-Delta Delta C(T)) method. Methods 25: 402-408, 2001.
25. Warren AY and Harrison D: WHO/ISUP classification, grading and pathological staging of renal cell carcinoma: Standards and controversies. World J Urol 36: 1913-1926, 2018.
26. Colaprico A, Silva TC, Olsen C, Garofano L, Cava C, Garolini D, Sabedot TS, Malta TM, Pagnotta SM, Castiglioni I, *et al*: TCGAbiolinks: An R/Bioconductor package for integrative analysis of TCGA data. Nucleic Acids Res 44: e71, 2016.
27. R Core Team (2012). R: A language and environment for statistical computing. R Foundation for Statistical Computing, Vienna, Austria. ISBN 3-900051-07-0, URL http://www.R-project.org/.
28. RStudio Team (2015). RStudio: Integrated Development for R. RStudio, Inc., Boston, MA URL http://www.rstudio.com/.
29. Rooney MS, Shukla SA, Wu CJ, Getz G and Hacohen N: Molecular and genetic properties of tumours associated with local immune cytolytic activity. Cell 160: 48-61, 2015.

30. Yu G, Wang LG, Han Y and He QY: ClusterProfiler: An R package for comparing biological themes among gene clusters. OMICS 16: 284-287, 2012.
31. Zhang HM, Yang FQ, Chen SJ, Che J and Zheng JH: Upregulation of long non-coding RNA MALAT1 correlates with tumour progression and poor prognosis in clear cell renal cell carcinoma. Tumour Biol 36: 2947-2955, 2015.
32. Hirata H, Hinoda Y, Shahryari V, Deng G, Nakajima K, Tabatabai ZL, Ishii N and Dahiya R: Long noncoding RNA MALAT1 promotes aggressive renal cell carcinoma through Ezh2 and interacts with miR-205. Cancer Res 75: 1322-1331, 2015.
33. Han Y, Liu Y, Zhang H, Wang T, Diao R, Jiang Z, Gui Y and Cai Z: Hsa-miR-125b suppresses bladder cancer development by down-regulating oncogene SIRT7 and oncogenic long non-coding RNA MALAT1. FEBS Lett 587: 3875-3882, 2013.
34. Malakar P, Shilo A, Mogilevsky A, Stein I, Pikarsky E, Nevo Y, Benyamini H, Elgavish S, Zong X, Prasanth KV and Karni R: Long noncoding RNA MALAT1 promotes hepatocellular carcinoma development by SRSF1 upregulation and mTOR activation. Cancer Res 77: 1155-1167, 2017.
35. Tripathi V, Shen Z, Chakraborty A, Giri S, Freier SM, Wu X, Zhang Y, Gorospe M, Prasanth SG, Lal A and Prasanth KV: Long noncoding RNA MALAT1 controls cell cycle progression by regulating the expression of oncogenic transcription factor B-MYB. PLoS Genet 9: e1003368, 2013.
36. Kim J, Piao HL, Kim BJ, Yao F, Han Z, Wang Y, Xiao Z, Siverly AN, Lawhon SE, Ton BN, *et al*: Long noncoding RNA MALAT1 suppresses breast cancer metastasis. Nat Genet 50: 1705-1715, 2018.
37. Li C, Miao R, Liu S, Wan Y, Zhang S, Deng Y, Bi J, Qu K, Zhang J and Liu C: Down-regulation of miR-146b-5p by long noncoding RNA MALAT1 in hepatocellular carcinoma promotes cancer growth and metastasis. Oncotarget 8: 28683-28695, 2017.
38. Yang L, Lin C, Liu W, Zhang J, Ohgi KA, Grinstein JD, Dorrestein PC and Rosenfeld MG: ncRNA- and Pc2 methylation-dependent gene relocation between nuclear structures mediates gene activation programs. Cell 147: 773-788, 2011.
39. Sun Z, Ou C, Liu J, Chen C, Zhou Q, Yang S, Li G, Wang G, Song J, Li Z, *et al*: YAP1-induced MALAT1 promotes epithelial-mesenchymal transition and angiogenesis by sponging miR-126-5p in colorectal cancer. Oncogene 38: 2627-2644, 2019.
40. Audibert A, Weil D and Dautry F: In vivo kinetics of mRNA splicing and transport in mammalian cells. Mol Cell Biol 22: 6706-6718, 2002.
41. Chen Q and Pollard TD: Actin filament severing by cofilin is more important for assembly than constriction of the cytokinetic contractile ring. J Cell Biol 195: 485-498, 2011.
42. Kanellos G, Zhou J, Patel H, Ridgway RA, Huels D, Gurniak CB, Sandilands E, Carragher NO, Sansom OJ, Witke W, *et al*: ADF and cofilin1 control actin stress fibres, nuclear integrity, and cell survival. Cell Rep 13: 1949-1964, 2015.
43. Pang D, Yang C, Li C, Zou Y, Feng B, Li L, Liu W, Luo Q, Chen Z and Huang C: Polyphyllin II inhibits liver cancer cell proliferation, migration and invasion through downregulated cofilin activity and the AKT/NF-κB pathway. Biol Open 9: bio046854, 2020.